

## Modeling Shrinkage Induced Micro-porosity

C.W. Hirt 11/19/03

Flow Science, Inc.

### Overview

Cast metal parts are sometimes unusable because they have internal gas pockets, or bubbles, which develop when the metal shrinks during solidification. A general term describing such bubbles or voids is “porosity.” When these bubbles are relatively large and localized the porosity is called **macro**-porosity. Prediction of macro-porosity in the interior of cast parts is a capability of most software packages currently used for the modeling of metal casting processes.

Another type of porosity, characterized by a more uniform distribution of small bubbles with a total average volume fraction on the order of one percent, is referred to as **micro**-porosity. This type of porosity is also caused by metal shrinkage during solidification, but its character is different from macro-porosity because it develops at a later stage in the solidification process. This distinction in types of porosity is important because each type requires a different modeling approach.

In this note we propose a new model that has been implemented in *FLOW-3D*<sup>®</sup> for predicting the occurrence of micro-porosity. The model is simple, requires only basic material property data, and adds virtually no noticeable CPU time to a solidification simulation. Best of all, the model is complimentary to macro-porosity models and may be used in conjunction with either a complete hydrodynamic shrinkage simulation that includes fluid flow or with simpler heat-transfer and shrinkage simulation having no fluid flow.

The new model has been checked using three sets of experimental test data. A final test, involving only qualitative results for the influence of pressure on micro-porosity formation has also been conducted.

### Review of Shrinkage Induced Macro-Porosity

There are several physical processes influencing volume shrinkage during solidification. Because liquid metal is nearly incompressible any loss in volume caused by shrinkage must be replaced by new liquid or by the opening of a void somewhere in the casting. The key to porosity formation is pressure. As metal cools it tends to a higher density because the thermal agitation of the molecules is less able to overcome the strong intermolecular forces pulling the molecules together. This shrinkage also reduces the metal pressure.

A reduction in pressure will draw in liquid metal to replace the volume loss to shrinkage provided there is liquid nearby that is able to flow. If the liquid cannot flow, internal void formation can occur when the pressure is lowered below the vapor pressure of the liquid, or more typically, below the vapor pressure of dissolved gases in the metal such as hydrogen. Strictly

speaking, the pressure must be somewhat lower than the vapor pressure to compensate for surface tension forces at a vapor bubble surface.

Whether or not liquid metal can flow in response to a lowering of the pressure depends on the degree of solidification. As liquid metal is cooled the first solid crystals begin to form at a temperature referred to as the **liquidus temperature**. Further cooling increases the fraction of solid versus liquid metal until all the metal is solid at a temperature called the **solidus temperature**. Experiments show that between the liquidus and solidus temperatures there some qualitative changes in the metal that must be accounted for in any realistic simulation of the solidification process.

For example, as the solid fraction increase from zero the apparent viscosity of the metal increases due to the solid particles (crystals) in the liquid, which are better able to transfer momentum than a pure liquid. Further, when sufficient solid has formed at the walls of the mold or die confining the metal, a flow resistance develops because the metal has difficulty penetrating the stationary crystal matrix (usually a cluster of dendritic arms). This point is called the **solid fraction for coherency**. Finally, when the solid fraction reaches a sufficiently high value for a dendritic structure to exist throughout the bulk of the metal, further liquid flow is virtually impossible without extremely high (generally unrealistic) pressure gradients. The zero flow point is called the **solid fraction for rigidity**, or sometimes, the **critical solid fraction**.

At solid fractions between the coherency and rigidity values the metal is subject to a flow resistance that is typically modeled as a type of flow in porous media, where the resistance is proportional to the degree of solidification (i.e., porosity). Examples of this type of model and some experimental data can be found in the article “Permeability for Flow of Interdendritic Liquid in Columnar-Dendritic Alloys,” by D.R. Poirier, Metallurgical Trans. B, p.245, Vol.18B, 1987.

In **FLOW-3D**<sup>®</sup> the user can input solid fraction values for coherency and rigidity that are appropriate for the material being modeled. The program will then apply a variable viscosity and D’Arcy drag resistance based on the computed values of solid fraction. These effects are automatically included in either of the two models available for the prediction of shrinkage induced macro-porosity. Those models are the hydrodynamic model with its full fluid flow capabilities and the simplified shrinkage model in which bulk fluid flow is only estimated. The simplified model requires much less computational effort and it is the best model choice when conditions are compatible with its underlying assumptions.

The weakest link in simulating macro-porosity is determining when liquid is (or is not) able to flow to compensate for volume shrinkage. The flow condition depends strongly on the flow resistance along pathways between the shrinkage location and reservoirs of liquid metal. Unfortunately, flow resistance as a function of solid fraction is not well known for any metal much less for specific alloys. Other weak links in modeling macro-porosity include the need for data describing the concentrations of dissolved gases in the liquid metal, their diffusion rates in the metal, and the saturation pressure-temperature relations for the gases. In practice, it is necessary to guess many of these things in order to perform a simulation. Fortunately, experience

has shown that approximations for these processes can give decent predictions for macro-porosity locations when the level of porosity is large enough.

For micro-porosity, on the other hand, the low volume fractions involved imply the need for highly accurate flow models (and material properties) if these approaches are to be effective. Alternatively, we must look for another type of model. This alternative is the subject of the present technical note.

### Shrinkage Induced Micro-Porosity

After metal has cooled enough for its solid fraction to exceed the point of rigidity there can be no (or very little) additional liquid flow to compensate for shrinkage. In aluminum A356, for instance, the solid fraction for rigidity is about 63% (see “Solidification Characteristics of Aluminum Alloys, Vol.3: Dendrite Coherency,” Arnberg and Bäckerud, American Foundrymen’s Society, Inc., 1996). This means that there is still 37% of the metal remaining to be solidified.

For the micro-porosity model that is proposed here we assume it is this last stage of solidification that accounts for micro-porosity. Support for this assumption comes from the observation that because the remaining liquid cannot easily flow through the dendritic crystal structure, the micro-porosity tends to be more uniformly distributed in small bubbles as opposed to the large void cavities associated with macro-porosity.

Because there is almost no information available for the level of pressure gradients necessary to have liquid flow in the solid fraction region above the rigidity point, we don’t want to use this mechanism in our simplified model. In fact, we don’t consider any fluid dynamic processes. The point of rigidity is just that, the point at which there can be no further metal flow in the usual fluid dynamic sense.

Since there is no flow, we cannot record the amount of micro-porosity in terms of the volume-of-fluid function that *FLOW-3D*<sup>®</sup> uses to identify metal-gas interfaces. Instead, we employ an independent scalar function to record the amount of porosity. Furthermore, because the micro-porosity is typically small it does not affect heat-conduction or heat-transfer processes in any significant way, which means that no changes are necessary to the solidification solver model.

Finally, the passive nature of this micro-porosity model means that it may be used in conjunction with macro-porosity models and with either a pure heat conduction simulation or with full hydrodynamic simulations that include filling and solidification processes.

### The Basic Micro-Porosity Model

Micro-porosity can only exist in a computational element containing a solid fraction exceeding the solid fraction for rigidity. In each such element a test is made to see if any of the adjacent elements that share a common face with the element have a solid fraction below the rigidity point. If one or more neighbors has a solid fraction less than the value for rigidity we assume that local liquid feeding is possible and no porosity is generated in the element. If all neighboring

elements exceed the solid fraction for rigidity then liquid feeding is not possible and the micro-porosity of the element is increased by the amount of shrinkage in that element during that time step.

The volume shrinkage,  $\Delta V$ , in an element is computed from the change in density using a conservation of mass relation,

$$(V_{old} - \Delta V)\rho_{new} = V_{old}\rho_{old}$$

where “old” means at the beginning of a time step and “new” means at the end of the time step. In this expression the density is evaluated in terms of the solid fraction.

A change in solid fraction is assumed directly proportional to the change in internal energy between the liquidus and solidus temperatures. At the liquidus point the metal is all liquid and at the solidus it is all solid. Although the solid fraction varies linearly with internal energy, it does not necessarily vary linearly with temperature.

Finally, we make the further assumption that the mixture density is a linear function of solid fraction,  $f_s$ ,

$$\rho(f_s) = \rho_{liq} + (\rho_{sol} - \rho_{liq})f_s$$

where  $\rho_{liq}$  is the density at the liquidus temperature ( $f_s=0$ ) and  $\rho_{sol}$  is the density at the solidus temperature ( $f_s=1$ ). Using the above two relations, the change in shrinkage volume,  $\Delta S$ , corresponding to the change in solid fraction,  $\Delta f_s$ , is

$$\Delta S = (1 - S)(\rho_{sol} - \rho_{liq})\Delta f_s / \rho(f_s)$$

Here  $S$  is the current micro-porosity volume fraction and  $f_s$  is the current solid fraction.

According to this expression, the maximum shrinkage porosity (volume fraction) possible is equal to  $(\rho_{sol} - \rho_{liq})/\rho_{sol}$ . However, the maximum micro-porosity is much less since it is associated only with solidification occurring above the critical solid fraction,

$$S_{max} = \frac{(\rho_{sol} - \rho_{liq})}{\rho_{sol}}(1 - f_{crit}).$$

Typically, this value is on the order of 1 to 2 percent for aluminum. For example, if  $\rho_{liq}=2.42$ ,  $\rho_{sol}=2.57$ , and  $f_{crit}=0.68$  then  $S_{max}=0.0187$  (1.87%).

## Extension of Model to Include Pressure Effect

It is well known that the application of a large pressure on a casting while it is solidifying can significantly reduce the amount of micro-porosity. One concept is that gas (or vapor) cannot form bubbles until the gas saturation pressure exceeds the ambient pressure. The process is essentially one of cavitation (or boiling). As the pressure of a material is reduced (or temperature increased) the saturation pressure of dissolved gas will eventually exceed the ambient pressure and bubbles will form.

In the present micro-porosity model we include pressurization in the following way. An initial pressure in the metal is set as an initial condition or from a filling simulation. Because we are only dealing with regions where the critical solid fraction is exceeded, the hydrodynamic pressure is no longer changing in these regions. As far as the new model is concerned, the pressure in each control volume can begin with any (positive) value.

As solidification proceeds, the pressure in an element is reduced because of metal shrinkage. The change in pressure is computed using a simple equation of state:

$$p = p_0 + a^2(\rho_{cr} - \rho(f_s))$$

The pressure  $p_0$  corresponds to the metal pressure when the solid fraction reaches the critical value for rigidity and the density is  $\rho_{cr}$ . Solidification increases the mixture density  $\rho(f_s)$ , which results in a reduction in metal pressure. The rate of reduction is proportional to  $a^2$ , which is the square of the speed of sound in the solidifying metal (i.e.,  $a^2 = dp/d\rho$ ). Alternatively,  $\rho a^2$  may be thought of as a bulk modulus for the metal.

No micro-porosity is allowed to form in a control element as long as its pressure, or the pressure of at least one of its neighbors, is greater than the saturation pressure.

Clearly, if  $p_0$  is large enough, and  $a^2$  is not too large, the pressure may never be reduced below the saturation pressure and no micro-porosity will occur.

In principle, we could invert the pressure equation to determine what value of  $f_s$  reduces  $p$  to the saturation value, and then use this value of solid fraction as an effective critical value that must be reached before feeding stops and micro-porosity can form. If  $p_0$  were constant, then simply increasing the critical solid fraction value to account for pressurization would be easy. For non-uniform  $p_0$ , however, the effective critical value would have to vary from one control element to the next, in which case it is just as easy to retain the pressure criteria as described.

A key to using this extension of the micro-porosity model is having a good value for  $a^2$ . Typical pressurization values are on the order of 10 atmospheres, while the maximum variation of  $\rho(f_s)$  for aluminum might be about 0.06 g/cc. To reduce the pressure to atmospheric (a change of nine atmospheres) the value of  $a^2$  would have to be equal to about  $1.67 \times 10^8$ , which gives an effective speed of sound equal to  $1.29 \times 10^4$  cm/s (423 ft/s). This value seems rather low since it is about 1/12 the speed of sound in water.

If we increase the value of the effective sound speed by a factor of two, still a low value, then  $a^2$  is increased by a factor of four and the change of solid fraction (density) necessary before the pressurization is eliminated is one fourth the total range. Correspondingly, the maximum micro-porosity that could form is only reduced to three fourths of the maximum value without pressurization.

Without good experimental data with which to make comparisons, it is not possible to assess this portion of the model. At the very least, it offers a mechanism that can be used to include the effects of pressurization with the constant  $a^2$  simply treated as an empirical parameter.

### Model Validation

All test cases use the aluminum alloy A356. A search was done of several sources (see references at end of paper) to obtain the material properties for this metal that are needed for performing simulations. The best data (chosen to cover the solidification range) are listed in the following table in CGS units with temperatures in degrees Celsius:

Liquidus Temperature	611.0
Solidus Temperature	555.0
Liquid Density	2.42
Solid Density	2.57
Liquid Specific Heat	1.19e+7
Solid Specific Heat	1.20e+7
Liquid Conductivity	0.7e+7
Solid Conductivity	1.3e+7
Liquid Viscosity	0.013
Solid Fraction for Coherency	0.23
Solid Fraction for Rigidity	0.68
Latent Heat of Fusion	4.25e+9

In addition, a non-uniform heat of fusion versus temperature was used. In the next table the first column is a temperature and the second column is the internal energy in the liquid-solid between that temperature and the previous temperature (the first value is the energy from absolute zero to the first temperature):

<u>CLTP (°C)</u>	<u>CLHT (erg/gm)</u>
555.0	6.66e+9
566.0	0.46e+9
572.0	2.28e+9
606.0	1.91e+9
611.0	0.67e+9

Energy values (CLHT) include the heat-of-fusion and the specific energy computed as the specific heat times the temperature change over the interval. The large values of energy at temperatures 572.0°C and 606.0°C arise from a large heat-of-fusion at a temperature of about 574.0°C, which means there is a rapid change in solid fraction at this temperature.

Finally, the sand properties used in all simulations were the same (in cgs units):

Thermal Conductivity	6.5e+4
Density times Specific Heat	1.7e+7
Heat Transfer Metal-to-Sand	2.0e+6

The first and second test cases were adopted from research performed in connection with the United States Consortium for Automotive Research (USCAR) Project. These cases involve a horizontal plate of A356 in a sand mold. One test had chill plates located at the end and on the top and bottom sides of the plate while the other has no chill plates. A third test case for which there is no data was a repeat of the USCAR plate test with varying levels of pressurization to show the qualitative effect of pressure on micro-porosity formation. Finally, the fourth test case was supplied by the University of Alabama, Birmingham and consists of a wedge of aluminum A356 cast in a gravity poured sand mold. A copper chill plate was located at the narrow end of the wedge to enhance solidification at that end.

The rectangular plate used in the plate tests is approximately 25.0cm long, 14.0cm wide and 3.2cm thick. Solidification over most of the plate can be treated as approximately one dimensional across the 3.2cm thickness. It is useful, in fact, to begin with this assumption because it gives a good picture of how the relative conductivities of metal, sand and chill affect the formation of micro-porosity.

### **One-Dimensional Test -- Sand**

The normal direction to the plate is taken to be the x direction. Metal extends from  $x=0$  to the center of the plate, a plane of symmetry, at  $x=1.6$ cm. Sand extends in the negative x direction from  $x=-5.5$ cm to  $x=0$  when there is no chill plate. When a chill plate is used it replaces the sand from  $x=-2.5$ cm to  $x=0$ .

First, let us consider the case with only sand. The ratio of the thermal conductivity of liquid metal to sand is about 108, which means that the variation in metal temperature across the plate should be very small during the solidification process. Temperature profiles in the metal at times 400, 800, 1200, and 1500s are shown in Fig.1 and confirm this observation. Because there is little spatial variation in metal temperature all the metal reaches the critical solid fraction at nearly the same time. This means that no region solidifying above the critical value is likely to have a neighboring region below the critical value that could feed shrinkage. Consequently, the micro-porosity should be at or near the maximum value possible, 1.87%. In fact, the simulation predicts, Fig.3, a value of 1.83% at the surface of the sand increasing linearly to 1.87% at the center of the plate.

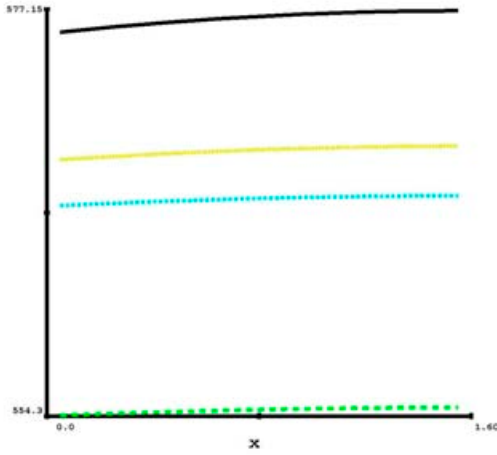


Figure 1. Metal temperature profiles for sand case at 400, 800, 1200, and 1500s (top to bottom) are seen to be nearly uniform across the (half) plate. Temperature scale from 554 to 577 °C.

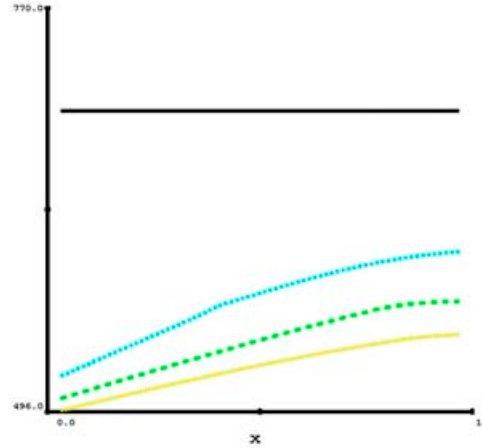


Figure 2. Computed metal temperature profiles with chill at 0, 10, 20 and 25s. Temperature scale from 496 to 770 °C.

### One-Dimensional Test – Chill Plate

When a chill plate is inserted between the metal and the sand (on top, bottom and end surfaces) a spatially uniform metal temperature is no longer possible and the solidification changes dramatically. In this case the chill plate was assumed to be gray iron with a density-specific heat product of  $4.23 \times 10^7 \text{ erg/cc}$  and a thermal conductivity of  $4.0 \times 10^6 \text{ erg/s/cm/K}$ , only slightly smaller than the conductivity of the metal. Computed temperature profiles in the metal at times 0.0, 10.0, 20.0, and 25.0s are shown in Fig.2.

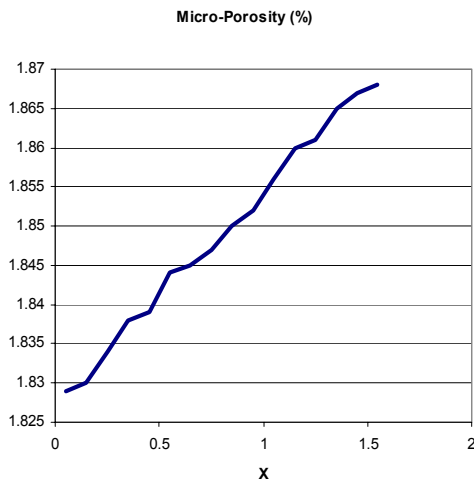


Figure 3. Micro-porosity in (half) 1D plate with sand. Computed porosity is nearly constant across the plate.

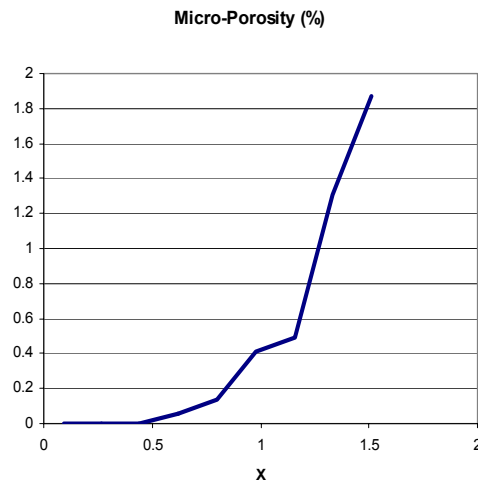


Figure 4. Micro-porosity in (half) 1D plate with chill. Porosity is zero at chill and maximum at center of plate.

Most obvious in this case is that complete solidification occurs in 25s compared to 1500s in the case without a chill. Furthermore the metal temperature has a definite gradient between the chill and plate center. Because of this distribution the micro-porosity also exhibits a distribution as shown in Fig.4.

There is zero micro-porosity near the chill where the cooling rate is largest, and the local temperature gradient in the metal is also large. In this region the metal reaches complete solidification before the adjacent metal reaches a critical solid fraction (and consequently is able to feed the shrinkage). At the center of the plate the situation is reversed. Metal adjacent to the center reaches the critical point before the center does and cannot provide feeding to the central region. As expected, without feeding, the center reaches the maximum possible level of micro-porosity.

Finally, it is worthwhile to use this simple test case to see what effect solidification properties have on the prediction of micro-porosity. In particular, what is the effect of assuming a linear relationship between solid fraction and temperature versus a non-linear relationship based on actual data (see previous table for CLTP-CLHT)? The effect, in fact, is substantial as seen in Fig.5. There is less micro-porosity when actual data are used.

This is also a good point at which to discuss an apparent short coming of the model. If the metal shrinks and the porosity is not at its maximum value, there must be some liquid flowing into the region to occupy some of the shrinkage volume. However, in the one-dimensional model there is no source for metal feeding. The problem is the simplicity of the model and the fact that it is passive and does not affect the actual flow processes. Since the amount of micro-porosity is always small, we have chosen to ignore actual flow details in favor of efficiency of computation. In the present model, and in contrast to macro-porosity models, no attempt is made to locate realistic liquid feeding paths. Instead, we only look at the state of adjacent grid elements to determine if feeding can occur.

These one-dimensional examples show the importance of cooling rates and corresponding temperature gradients in the development of micro-porosity. Extending them to three-dimensions only adds a few details at the lateral boundaries of the plate.

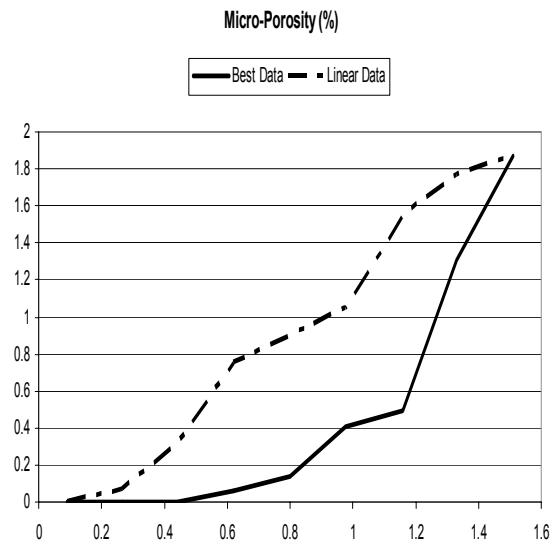


Figure. 5. Comparison of micro-porosities in (half) 1D plate with chill. Significantly smaller porosities (solid line) are computed with best material property data as compared to linear temperature vs. solid-fraction relation (dashed line).

### Three-Dimensional Plate

Figures 6 and 7 show the computed micro-porosity distribution along the centerline of the plate with just sand and with a chill, respectively. In addition, the corresponding experimental data obtained in the USCAR project are also indicated. The experimental values were obtained by making vertical cuts across the long axis of the plate and then measuring the average micro-porosity over a region at the center of the plate that extended from the top to bottom surface and had a width of at least 1cm (see A.S. Sabau and S. Viswanathan, "Microporosity Prediction in Aluminum Alloy Castings," Metallurgical and Materials Trans., Vol.33B, p.243, 2002). A similar region average has been used for the computational data.

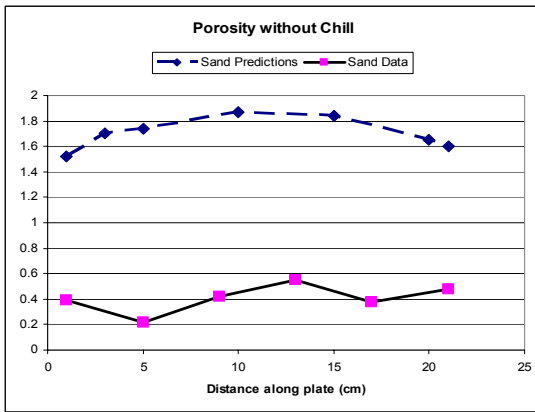


Figure 6. Comparison of computed (dashed line) and measured micro-porosity (solid line) along axis of plate in pure sand mold.

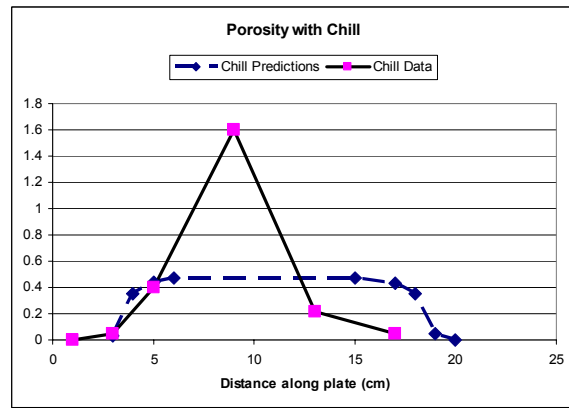


Figure 7. Comparison of computed (dashed line) and measured micro-porosity (solid line) along axis of plate with chill in mold.

In the sand mold case, Fig.6, both predictions and data exhibit a nearly constant micro-porosity along the plate, however, the averaged computed value of approximately 1.8% is much larger than the averaged measured value of about 0.4%. The computed results also indicate somewhat smaller values at the ends of the plate where the initial cooling rate is larger. This trend at the ends makes sense but is not seen in the measured data.

With the chill case, Fig. 7, we see good qualitative agreement at the ends of the plate where the micro-porosity tends to zero. This agreement is particularly good near the zero coordinate end of the plate where the computational predictions are nearly right on the experimental data for the first 5cm. The experimental data point at 9cm appears anomalous. One would expect the micro-porosity along the middle of the plate axis to be uniform (i.e., there is no geometric or other obvious reason for a variation to exist). In this connection it is useful to note that the computed micro-porosity distribution predicts zero porosity over most of the cross section of the plate, but with a large porosity occurring at the very center. This would be expected because of the rapid cooling caused by the chill plates. Away from the central region liquid in the center feeds the shrinkage of the metal lying closer to the chill plates. Once the solidification front has reached the center of the plate, however, no feeding is possible and a nearly maximum micro-porosity develops there. Because of this large variation in porosity over the cross section of the plate, it is possible that the area-averaging technique used in the experiments could have resulted in large

fluctuations in the measured porosity values. Such an explanation could explain the anomalous looking results. In fact, if the point at 9cm is eliminated the agreement between experiment and calculation looks quite good.

Overall the computed results show good qualitative results, but quantitatively they could be better. Some of the discrepancy in values may be the result of the area-averaging technique used to measure micro-porosity. No error levels were reported for the experimental test data, so there is no information available to determine how reliable it is. As noted previously, there is some reason to believe that the reported data may not be entirely reliable. For this reason we can justify some disagreement in quantitative comparisons with the plate data.

### **Reducing Micro-Porosity with Pressurization**

The USCAR plate test case is a simple arrangement that we can use to demonstrate the influence of pressurization on the micro-porosity. For test purposes we assume that porosity cannot form until the pressure in the metal drops below one atmosphere. We also assign an effective sound speed to the metal that is one tenth the speed of sound in water,  $a=1.554e5\text{cm/s}$ . Such a low speed probably cannot be justified although it is not unreasonable to assume the speed would be less than the speed of sound in liquid aluminum because of two-phase effects (i.e., solid particles in the liquid).

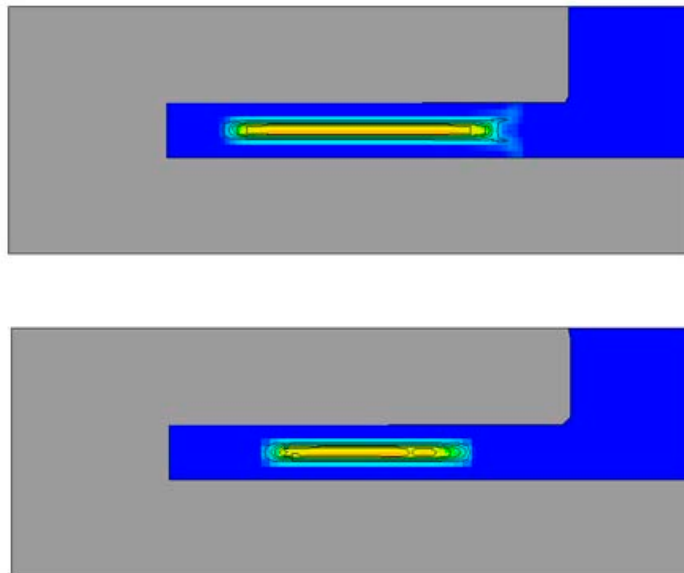


Figure 8. Comparison of micro-porosity in central plane of plate when no pressurization is assumed (top) versus a ten atmosphere initial pressurization (bottom).

In Fig.8 we compare micro-porosity distributions in a vertical cut through the long axis of the plate. A portion of a riser is at the right hand side of the plate. The top frame is the micro-porosity from the original simulation that had no pressure effects, while the bottom frame shows the micro-porosity with a 10 atmosphere initial pressurization. Clearly there is reduced porosity with pressurization. Not only is the size of the region containing micro-porosity reduced but the maximum value at the center is also reduced from 1.87% to 0.35%. With a 20 atmosphere initial

pressurization no micro-porosity was computed to form. These simple tests qualitatively show that the effects of pressurization on micro-porosity are captured by the new model.

### Three-Dimensional Wedge Test

The last test case, provided by the University of Alabama, Birmingham, is that of a wedge with its thin edge aligned vertically, Fig. 9. For this casting there were thermocouple measurements of temperature histories at three locations in the center of the wedge (5.0, 15.24, and 22.86cm from the thin end). A comparison of computed and experimental temperatures is given in Fig.10. Solidification is complete when the metal temperature reaches 555°C. There is good agreement at all three locations for temperatures at or above the solidus temperature, which is the only temperature region we are interested in for this study. At lower temperature the measured data is significantly higher than that computed and even seems to be leveling off to a very slow decay. This suggests that further thermal shrinkage of the solid metal may be pulling the metal away from the sand causing an insulating layer of air to form and reduce heat transfer to the sand.



Figure 9. Wedge with riser and sprue. Chill plate is placed in sand mold at its thin end.

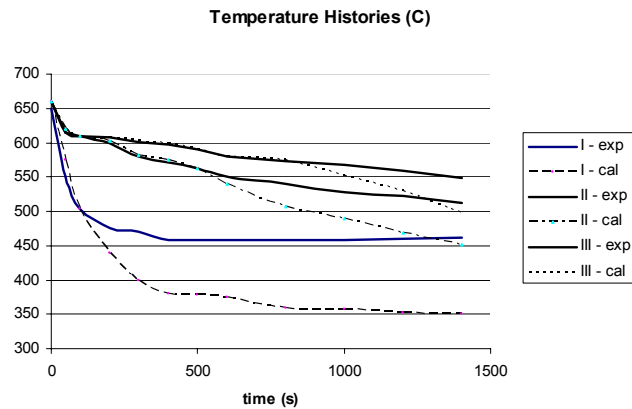


Figure 10. Temperature histories at three locations in the center of the wedge. Computed data is dashed and solid data is from thermocouple measurements. Agreement is quite good at all locations above the solidus temperature of 555C.

Using the same physical data as that used for the plate examples (the wedge is also A356 aluminum) a simulation was performed for one symmetric half of the wedge and riser. The runner and sprue were not included in the simulation. Figure 11 shows the computed micro-porosity along a center line in the wedge together with the measured micro-porosity. Although the computed values are consistently lower the general agreement is quite good. Both measured and computed values are zero near the chill end, and both exhibit maximum values at the thick end of the wedge. These limits are what would be expected. The computed values plotted in Fig. 11 are those along the wedge center line and have not been area-averaged.

From the computational results one can observe that center line values of micro-porosity are somewhat smaller than values closer to the surfaces of the wedge. This is contrary to the plate

tests and indicates the importance of geometry. For the plate the central region is more nearly one-dimensional between the top and bottom surfaces. This leads to a more uniform solidification (smaller solid fraction gradient) and larger micro-porosity in the center. For the wedge, however, the small dimension is that between the diverging faces and that divergence results in a larger solid fraction gradient at the center and a smaller micro-porosity.

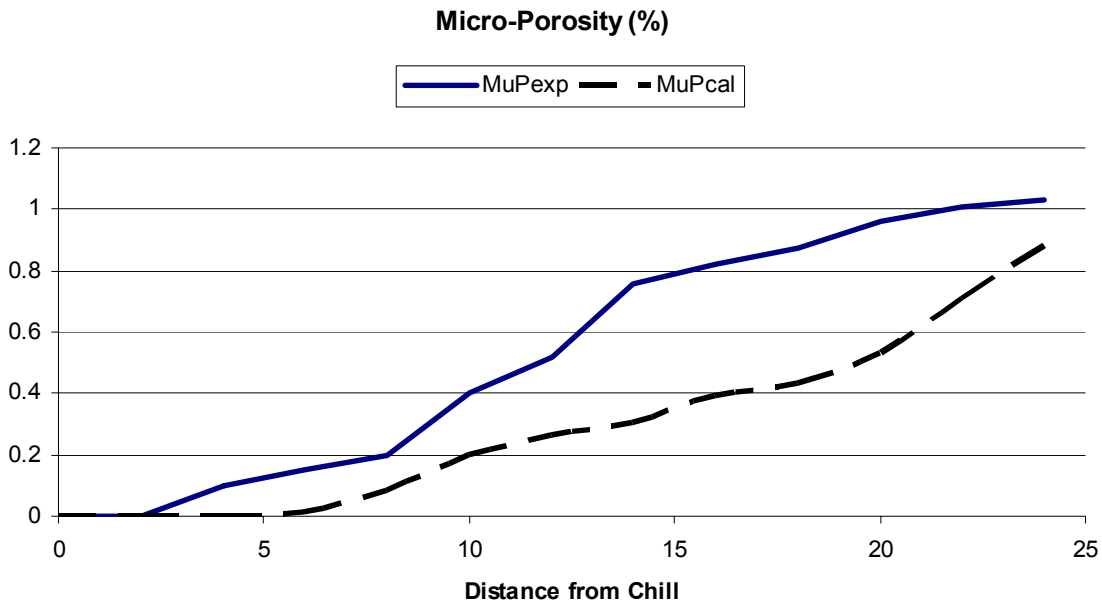


Figure 11. Micro-porosity measured (solid line) and computed (dashed line) in wedge.

### Summary Comments

A simple model has been incorporated into *FLOW-3D*<sup>®</sup> for the prediction of micro-porosity. This model is passive so it does not affect other models in the program. In particular, it can be used to supplement the macro-shrinkage (macro-porosity) model. Very little data is needed to use the model, but the computed results do depend on the physical data specified for the metal. Most important are the metal densities at the liquidus and solidus temperatures and the critical solid fraction (solid fraction for rigidity). This data controls the maximum amount of micro-porosity that can form.

If data is available for the relationship between heat-of-fusion and temperature in the solidification region, then this should be included in the simulations to improve the predictions.

The model has been tested against three experimental data sets. Two tests involved a rectangular plate and one involved a wedge. The model produces consistent approximations for all cases. It gives good qualitative distributions and very reasonable quantitative results.

In some ways the present micro-porosity model is similar to a temperature and temperature-gradient functional criteria method for estimating shrinkage induced micro-porosity. For example, whether or not a given control volume will experience an increase in porosity depends

on its state (temperature or solid fraction) and the state of the neighboring elements (local temperature and/or solid fraction gradients). On the other hand, what distinguishes this model from simple functional criteria is that it integrates these effects over the full range of solidification rather than making a single evaluation at some specified temperature or solid fraction value. Furthermore, because the model is incremental, it's possible (though not likely) for control volumes to solidify, melt, and re-solidify. Also, a pressure effect has been included in the model that is generally not a part of a simple temperature-gradient method. On balance, then, the new model offers significant improvements over function-criteria predictions.

Everything considered, it is hoped that the new micro-porosity model will prove useful to users of *FLOW-3D*<sup>®</sup>.

#### Appendix – Sources for Material Property Data

1. "Solidification Characteristics of Aluminum Alloys," Vol.3: Dendrite Coherency, L. Arnberg and L. Bäckerud, American Foundrymen's Soc., Inc. 1996.
2. Metal Casting Data from the web:  
[http://metalcasting.auburn.edu/data/A356\\_Aluminum/A356.html](http://metalcasting.auburn.edu/data/A356_Aluminum/A356.html)
3. "Recommended values of thermophysical properties for selected commercial alloys," K.C. Mills, National Physical Laboratory, Woodhead Pub. Ltd., 2002.